Rapid 1024-Pixel Electrochemical Imaging at 10,000 Frames Per Second Using Monolithic CMOS Sensor and Multifunctional Data Acquisition System

Kevin A. White, Geoffrey Mulberry, and Brian N. Kim

***Abstract*— Fast electrochemical imaging enables the dynamic study of electroactive molecule diffusion in neurotransmitter release from single cells and dopamine mapping in brain slices. In this paper, we discuss the design of an electrochemical imaging sensor using a monolithic complementary metal–oxide–semiconductor (CMOS) sensor array and a multifunctional data acquisition system. Using post-CMOS fabrication, the CMOS sensor integrates 1024 on-chip electrodes on the surface and contains 1024 low-noise amplifiers to simultaneous process parallel electrochemical recordings. Each electrochemical electrode and amplifier is optimized to operate at 10.38-kHz sampling rate. To support the operation of the high-throughput CMOS device, a multifunctional data acquisition device is developed to provide the required speed and accuracy. The high analog data rate of 10.63 MHz from all 1024 amplifiers is redundantly sampled by the custom-designed data acquisition system which can process up to 73.6 MHz with up to ∼400 Mbytes/s data rate to a computer using universal serial bus 3.0 interface. To contain the liquid above the electrochemical sensors and prevent electronic and wire damage, we packaged the monolithic sensor using a 3-D printed well. Using the presented device, 32 pixel × 32 pixel electrochemical imaging of dopamine diffusion is successfully demonstrated at over 10,000 frames per second, the fastest reported to date.**

***Index Terms*— Amperometric sensors, biomedical transducers, biosensors, electrochemical devices.**

I. Introduction

ELECTROCHEMICAL sensor arrays offer a high spatiotemporal resolution in the study of redox molecule diffusion dynamics, including amperometric recordings of neurotransmitter release at the single-cell level [1], electrochemical imaging of dopamine in brain slices to map the H_2O_2 level that associates with neurological diseases [2] and dopamine level which can help study Parkinson's Disease [3], and electrochemical imaging of biofilms [4], [5], glucose [6], and acetylcholine [7]. In electrochemical recordings, the redox molecules can either oxidize, releasing electrons into the electrode that can be measured as negative electrical current, or can induce reduction by taking electrons from the electrode to cause positive current into the electrode. The measurement of electron transfer by electrochemical reaction can be fast, milliseconds to microseconds in temporal resolution, and thus has a unique advantage in capturing the fast dynamics of redox molecule diffusion. Also, the electrochemical recordings can be highly sensitive and specific to electroactive molecules. With high temporal resolution and sensitivity, recent developments have focused on parallelization and miniaturization of sensors and electronics [8]. An array of sensors can be developed to offer simultaneous detection from many electrodes in parallel. In such parallel recordings, the geometric arrangement of the sensor array can be used to construct a spatial resolution from the set of recordings. These measurements require the aforementioned array of electrodes as well as an array of readout circuits to amplify and process the signal originating from each electrode. Large parallel recordings of electrochemical signals impose challenges in developing such instrumentation. For an array with a channel count beyond 1000, the use of commercially-available amplifiers is costly and the direct connection of individual electrodes to their respective amplifier using wiring is impractical. Recently, using microtechnology to manufacture complementary metal-oxide-semiconductor (CMOS) chips has been investigated as an option to scale up the number of parallel recordings to develop a programmable CMOS 5 × 10 electrochemical sensor array [8], an array of 59,760 electrodes to provide up to 2048 concurrent recordings [9], [10], a monolithic CMOS sensor with 100 on-chip electrodes and 100 parallel recordings [1], a 16 × 16 pixel array on an integrated CMOS device with a frame rate of up to 333 frames per second to study time-varying mixing and diffusion rates of ions [11], and an electrochemical imaging sensor with a 32 × 32 sensor array that produces 90 frames per second [12]. By directly integrating the electrode array on the CMOS chip, the bulk of interconnects can be eliminated and the large-scale integration (LSI) of circuits can be used to integrate a large array of amplifiers and readout circuits in a small silicon chip.

Manuscript received April 24, 2018; accepted May 10, 2018. Date of publication May 14, 2018; date of current version June 12, 2018. This work was supported by the National Science Foundation under Grant #1745364. The associate editor coordinating the review of this paper and approving it for publication was Dr. Cheng-Ta Chiang. *(Corresponding author: Brian N. Kim.)*

K. A. White and G. Mulberry are with the Department of Electrical and Computer Engineering, University of Central Florida, Orlando, FL 32816 USA (e-mail: kwhite64@knights.ucf.edu; gmulberry@knights.ucf.edu).

B. N. Kim is with the Department of Electrical and Computer Engineering, University of Central Florida, Orlando, FL 32816 USA, and also with the Burnett School of Biomedical Sciences, College of Medicine, University of Central Florida, Orlando, FL 32827 USA (e-mail: brian.kim@ucf.edu).

Digital Object Identifier 10.1109/JSEN.2018.2835829

Using an integrated monolithic CMOS sensor still requires an external data acquisition system to enable the complicated functions of the sensor device as well as to record and transfer data into a computer for further analysis. High-performance data acquisition systems add a substantial amount of cost and size to the instrumentation and limits portable applications. The presence of integrated analog-to-digital converters (ADC) in the CMOS sensor can simplify the external acquisition system. However, because monolithic CMOS sensors make direct contact with the biological and/or chemical substance being interrogated, such sensors are generally disposable and intended for single-use. Thus, the use of external ADCs is often more cost effective than integrating ADCs, which occupy a large area in the in the CMOS device, driving up the cost of the disposable devices. With high-throughput applications such as electrochemical imaging, the data acquisition needs to support fast digitization and large data transfer. For example, supporting the operation of a 1,000-pixel electrochemical imager with 10,000 frames per second requires a 10 MHz ADC sampling rate which results in 20 Mbytes/s (MB/s), assuming 2 bytes per sample for 16-bit ADCs. This transfer rate can easily multiply by a factor of two or more depending on redundant sampling for accuracy and noise [1]. Commercially-available high-performance data acquisition systems are costly with limited options and are unavailable for applications requiring fast sample rates over 100 MS/s and high accuracy 16-bit resolution. Previously, other data acquisition systems have been presented as an alternative to the costly commercially-available acquisition systems [13]–[17] improving sampling capabilities and cost effectiveness. Previous studies have proven the low-cost and portable capabilities of data acquisition systems using Arduino [13], custom-designed PCBs [14], and FPGAs [16], [17], but they are insufficient for many high-throughput applications that require high temporal resolution. For high-throughput applications, the data transfer rate is limited by the selected interface. Common interfaces for fast data transfer are peripheral component interconnect (PCI), PCI Express (PCIe), and universal serial bus (USB). Among those interfaces, USB connection is easy to use and is widely available in almost all computers and laptops. For the ubiquitous USB interface, the transfer rate for USB 3.0 is 5 Gbits/s. Using USB connectivity for such data acquisition systems widens the usability of the system which would have been limited to sophisticated research laboratories. The high-power delivery of USB interfaces from 4.5 W (USB 3.0) to 15 W (type-C) can be used for portable applications by designing a data acquisition system to rely exclusively on USB power. As high-throughput data acquisition is becoming more vital in biotechnology to enable multichannel brain-machine interfacing [18], high-throughput screening (HTS) for drug studies [19], [20], high-throughput electrophysiology recordings [1], and next-generation sequencing [21], USB connectivity introduces a low-cost, simple, and portable option.

In this paper, the comprehensive design of a 1024-pixel electrochemical imaging sensor and multifunctional data acquisition system is presented. In Section II, we describe the design of the monolithic CMOS-based electrochemical sensor. In Section III, we discuss the design and characterization of the multifunctional data acquisition system with 32 parallel ADCs to support the measurements from the CMOS-based sensor. In Section IV, we analyze and characterize the high-performance data acquisition system in conjunction with the CMOS sensor. In Section V, we describe a dopamine diffusion mapping experiment using the comprehensive electrochemical imager, consisting of the monolithic CMOS device and the multifunctional data acquisition system.

II. Monolithic CMOS Electrochemical Sensor

Neurotransmitters, such as dopamine, can be oxidized at an electrochemical electrode and the released electrons can be directly measured (Fig. 1). A CMOS device is designed with on-chip electrodes to measure the electrochemical signal directly on the chip (Fig. 1a). Two-dimensional electrochemical imaging of dopamine diffusion can be performed by using a CMOS device with an array of on-chip electrodes which can probe the electrochemical signal at multiple locations simultaneously (Fig. 1b). The electrochemical current can be recorded using a transimpedance amplifier (TIA). The recording of a small current and the processing of the signal are performed on the CMOS device. For this purpose, we used an integration capacitor-based TIA design. The current signals, ranging from pA to nA, injected into the electrodes are measured by the TIAs integrating capacitor. The voltage change in the capacitor is read out at a certain interval using correlated double sampling (CDS). The voltage readout is followed by a reset phase to recharge the capacitor using a parallel switch (Fig. 1c). Each TIA consists of an operational amplifier (OPA), an integrating capacitor (51 fF), a compensation capacitor (20 fF), a 1-bit SRAM, and additional transistors for testing and readout functionality within a 30×30 μm area (Fig. 1c). The transimpedance gain of each TIA is set to 0.54 mV/pA. The noise level for the TIA is measured to be 470 fA_{RMS} at 10 kHz sampling rate with a $\sim$4.4 kHz bandwidth. A time-division multiplexing technique, which staggers the integration period of each amplifier to remove any dead time in recordings due to readout, is adapted and results in the parallel recordings of 1024 electrodes [1]. The array of 1024 TIAs is arranged with 32 columns $\times$ 32 rows (Fig. 2a). In a column with 32 electrode-amplifier pairs, all of the current integrated voltages are time-division multiplexed into a single output, thus providing all 1024 electrode recordings through 32 parallel outputs. This output is fed to an output driver which consists of a unity-gain OPA followed by an nMOS source follower, which drives the output pins of the CMOS device and a load (the input impedance of the external ADC). The timing circuity relies on external clock sources to generate all the clocks required to operate the TIAs and multiplex the 1024 outputs. The timing circuits are designed primarily using traditional transmission gate D flip-flops. The analog outputs and digital inputs for the chip are interfaced with the external multifunctional data acquisition system (Fig. 1c), which will be described in Section III. The CMOS device is designed and simulated using the Cadence Virtuoso Analog Design Environment. The CMOS chip is fabricated using a standard 0.35 μm CMOS foundry process and the die size

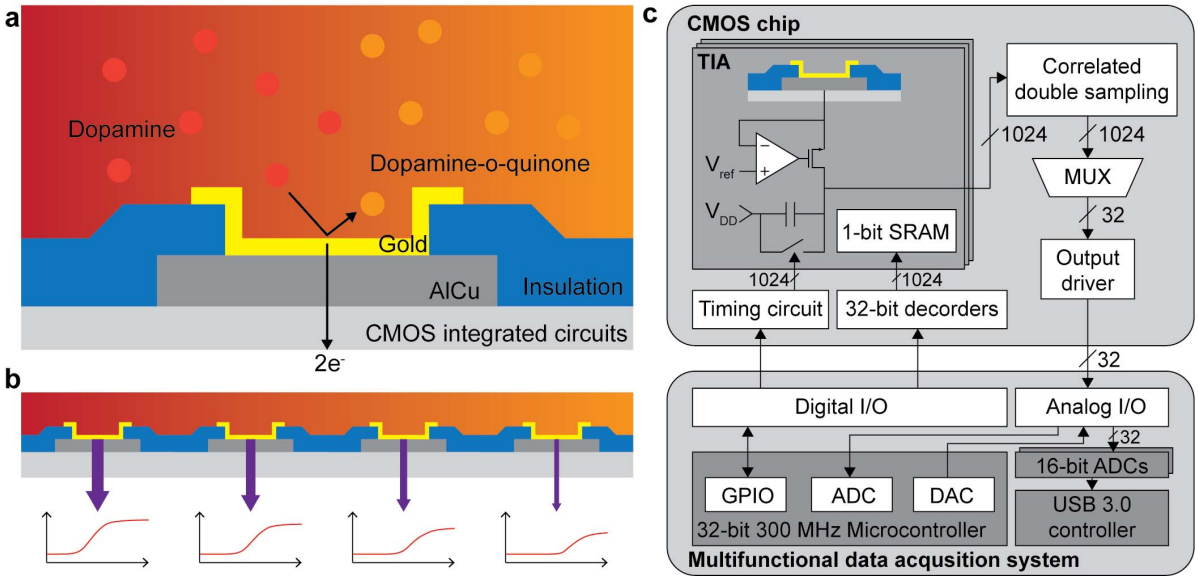

Fig. 1. Monolithic CMOS electrochemical imaging sensor. (a) Monolithic integration of gold electrodes on a CMOS device can be used to directly oxidize dopamine to dopamine-o-quinone, which results in electrons transferred into the integrated circuits. (b) Using the scalability of the circuits and on-chip electrodes, multiple electrode-amplifier pairs can record electrochemical signals simultaneously. Individual recordings can be used to study the dynamics and diffusion of electroactive molecules. (c) System design of the monolithic electrochemical imaging sensor using a CMOS chip and external data acquisition system.

TABLE I
SPECIFICATIONS OF THE CMOS ELECTROCHEMICAL SENSOR

Properties	Specifications
Technology node	0.35 µm
Die size	5 mm × 5 mm
Number of electrodes	1024
Number of amplifiers	1024
Design area per amplifier	30 µm × 30 µm
Electrode size	15 µm × 15 µm
Noise performance	470 fA_{RMS}
Transimpedance gain	0.54 mV/pA
Bandwidth	~ 4.4 kHz
Sampling rate per channel	10 kHz
Accumulated Sampling rate	~10 MHz
Electrochemical frame rate	~ 10,000 frames/s
Total power consumption	12.5 mW

is 5 mm × 5 mm, and the detail specifications are provided in Table I.

Electrochemical recordings require a polarizable electrode,including gold or platinum, to exhibit a high signal-to-noise ratio in measuring oxidative current without background current due to chemical reaction of the electrode itself [22]. However, standard CMOS foundries do not offer polarizable metals in the manufacturing process. Thus, post-CMOS fabrication is performed to monolithically integrate an electrode array on the surface of the CMOS chip. Each chip, fabricated from the foundry, is processed using photolithography to accomplish gold patterning through a lift-off process. Initially, the die is attached to a coverslip (25 mm × 25 mm) to ease the handling of the small substrate. The die is cleaned using acetone, isopropanol (or methanol), and DI water. A negative photoresist layer using NR9-1500PY is patterned, followed by sputtering of 15 nm Ti and 150 nm Au (Fig. 2b). Lift-off is then achieved by rinsing the die with acetone. Each gold electrode pattern is ~ 15 μm × 15 μm and is connected directly to its respective amplifier through a small insulation opening (Fig. 1a). After the photolithography process, the CMOS chip is bonded to a custom PCB that allows for the insertion of the CMOS device into a socket. This allows for the same experimental setup to be used with other CMOS chips with ease. The CMOS chip is wire-bonded to this custom PCB and a plastic well is used to protect the wire-bonds from liquid contact (Fig. 2c). The well is 3D-printed out of ABS plastic and coated with a layer of PDMS, for waterproofing and biocompatibility. The well is then bonded to the custom PCB and CMOS chip using additional PDMS (Fig 2d). The well has a small opening in the center to allow access to the surface of the CMOS chip as shown in Fig. 2e.

III. MULTIFUNCTIONAL DATA ACQUISITION SYSTEM

The multifunctional data acquisition board is used to operate the monolithic CMOS electrochemical sensor (Fig. 3). The multifunctional data acquisition board provides key capabilities to enable high-throughput applications, including 32-ch 16-bit resolution analog recordings, 16 digital inputs and outputs (I/O), 2-ch 12-bit analog recordings, 2-ch 12-bit analog outputs, and 400 MB/s data transmission over USB 3.0. The system uses a custom-designed PCB and a Cypress FX3 board (Fig. 3).

A. Design of Multifunctional Data Acquisition System

The Atmel SAME70 32-bit microcontroller unit (MCU) functions as the control center for the data acquisition system

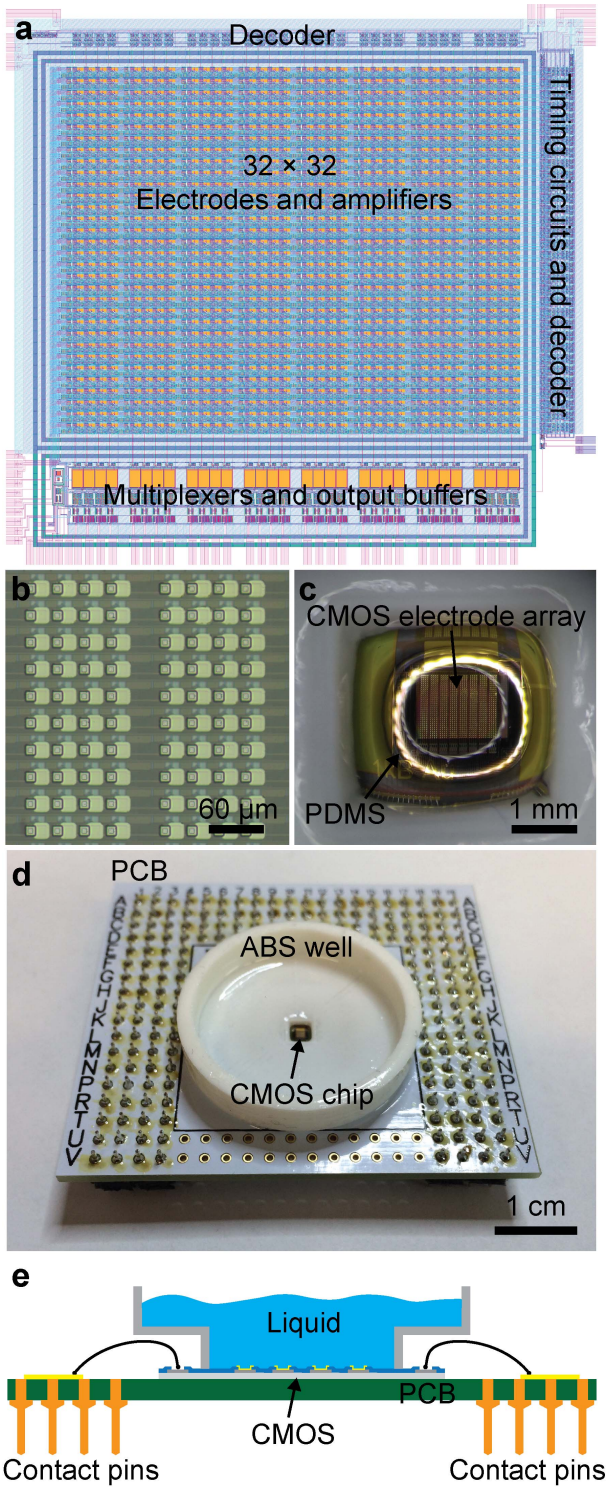

Fig. 2. Post-CMOS processing and packaging of the monolithic sensor. (a) The layout for the 1024-ch CMOS electrochemical sensor. (b) On-chip gold electrode array with each electrode size of ~15 μm × 15 μm. (c) The CMOS chip is packaged using a 3D-printed ABS well and PDMS, leaving a small opening on the electrode array. (d) The packaged chip on a custom-designed PCB. (e) The cross-sectional diagram of the packaged chip where the 3D-printed well contains the liquid above the electrode array and prevents liquid contact to the wire bonds and other electronic components.

and receives commands from a computer through the serial USB port (Fig. 4). The chip generates all of the clock signals required for the ADCs and USB 3.0 controller to operate

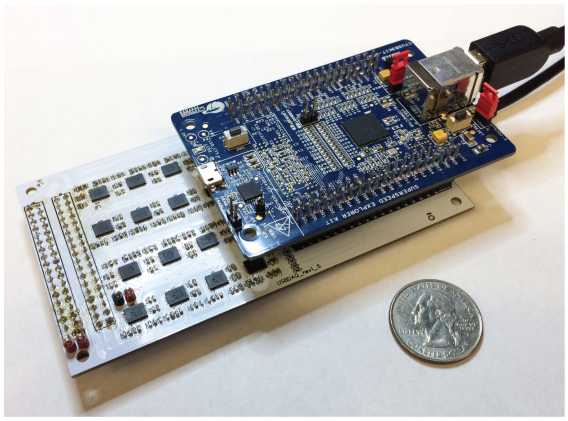

Fig. 3. The multifunctional data acquisition system. The system consists of a custom-designed PCB (white board) and a USB 3.0 controller board (navy board). The system is capable of 32-ch simultaneous analog recordings with digital I/O and analog output functionalities and can transmit up to 400 MB/s of data over USB 3.0.

synchronously as well as any clock signals required for external devices to operate in sync with the data acquisition system. The MCU chip also provides additional ADCs, digital I/O, and waveform generation using the embedded digital-to-analog converters (DACs).

There are 16 ADC chips (LTC2323-16, Linear Technology) used in the presented data acquisition system. Each ADC chip has two embedded ADCs with an individual maximum sampling rate of 5 MHz, providing a total of 32 high-speed 16-bit ADCs. The board is designed without anti-aliasing filters to offer flexibility in the sampling bandwidth. For each application, appropriate anti-aliasing filters are attached directly to the I/O interface of the data acquisition board. These ADCs convert the 32 parallel analog inputs from the CMOS chip to their 16-bit serial digital representations. The parallel output streams of the 32 ADCs are connected directly to 32 parallel general purpose I/O (GPIO) pins on the USB 3.0 board through the USB 3.0 interface pin headers. The USB 3.0 controller is used to transfer the large amounts of data acquired from the ADCs to a computer with high-throughput. The USB controller accumulates data in its embedded first in, first out (FIFO) memory and transfers data to the connected computer in packets at a rate up to 400 MB/s. The overall size of the system is 13 cm × 6.3 cm × 3 cm and weights 79.7 g. The system operates using the USB 5.0 V power, and thus can be used for portable applications in conjunction with a laptop.

B. Embedded Programming and Software

The firmware loaded into the USB 3.0 controller is designed to achieve a slave FIFO interface. This firmware configures the controller to receive a clock signal for synchronous operation from the MCU, record the parallel outputs from the high-speed ADCs, and send packets of data through the USB interface. A data streamer application is created to control the streaming of data from the USB controller to a computer. Additionally, a LabVIEW program is created to execute this streamer application and simply requires the user to start data transfer from the ADCs to the computer. This LabVIEW program

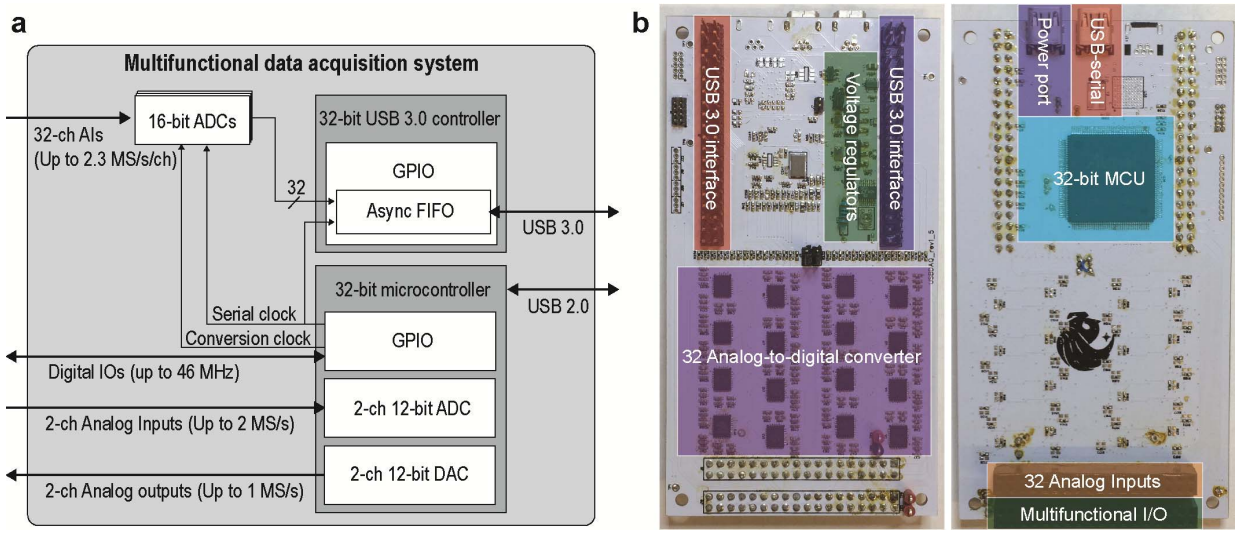

Fig. 4. Functional blocks and photographs of multifunctional data acquisition system. (a) The system diagram of the data acquisition system consisting of 32 16-bit ADCs, 16 fully-customizable digital I/Os, additional 2-ch ADCs, and 2-ch DACs. The USB 3.0 controller transmits data to the computer at high-speed and the 32-bit MCU communicates with the computer to receive commands for various configurations. (b) The PCB of the acquisition system consisting of 32 ADCs, USB 3.0 interfaces for USB board connection, the 32-bit MCU, voltage regulators, and a versatile I/O interface of 32 analog inputs and multifunctional I/Os.

specifies where the data is saved by the streamer application and the settings for the streamer are preset for optimal data throughput. The firmware programmed into the MCU provides the capability to operate and activate the multifunctionality of the data acquisition system. When powering up, the MCU will first configure its internal clocks to become operational. After this initialization, the MCU waits for the chip to receive a command from the computer. An MCU LabVIEW interface is developed to provide a user interface for controlling the MCU. This program allows the user to communicate with the chip through the USB serial port and tailor the functionality of the available pins to their needs. Each digital I/O can be individually set, the waveforms generated by the DACs can be changed, and the MCU embedded ADCs can be used for additional analog sampling.

IV. Analysis of High-Performance Data Acquisition

The simultaneous recording and multifunctional capabilities of the data acquisition system are tested by operating the high-throughput CMOS sensor, which demands both a fast-analog acquisition rate and a high channel count. The CMOS device has 32 analog outputs, and each output requires at least a 1.3 MHz sampling rate from the ADC to effectively resolve all of the multiplexed data. The external clock sources required for the CMOS device are generated by the MCU.

A. Simultaneous 32-ch Analog Recordings at 1.3 MHz Sampling Rate Per Channel

For this test, 332 kHz analog test pulses are generated by the CMOS device and the amplitude of the analog pulses varies between 1 – 2 V. The ADCs are configured to operate at 1.3 MHz per channel and the 32 individual analog signals are successfully recorded in parallel using the 32 ADCs in the system (Fig. 5). The USB 3.0 controller is set to operate with a 26 MHz peripheral clock (PCLK) which determines the digital sampling rate. Because each data package of the 32-bit USB controller is 4 bytes, the resulting transfer rate from the USB controller is ~100 MB/s. The data acquisition is stable for long-term continuous recordings and is mainly limited by the size of the computer's hard drive. With the 1.3 MHz per channel sampling rate, a one-minute recording results in a 6.24-Gbyte binary file.

B. Performance and Noise Characteristics

For this test, a 2-pole anti-aliasing filter with a cutoff frequency of 530 kHz is attached in the I/O interface of the data acquisition system to minimize aliasing noise. The system is tested with two different ADC sampling rates, 1.3 MHz, and 2.3 MHz, and a reference voltage is recorded using each sampling rate to analyze the performance and the noise characteristics. The recorded noise spectral densities (NSD) are shown in Fig. 6. The measured noise densities are 1.01×10^{-12} V^2/Hz and 4.58×10^{-12} V^2/Hz for 1.3 MHz, and 2.3 MHz, respectively, which are suitable for the electrochemical imaging application.

V. Electrochemical Imaging of Dopamine Diffusion

The setup for the electrochemical imaging is shown in Fig. 7. The setup consists of the multifunctional data acquisition system, monolithic CMOS sensor, biasing board for the CMOS device, and a 3D-printed microscope mount for the system. Each CMOS-based electrochemical electrode measures the oxidation current at 10.38 kHz sampling rate, and thus, the parallel recording from the 1024 electrode array sums to a total sampling rate of 10.63 MHz sampling rate. Each ADC samples with four times redundancy, thus the total

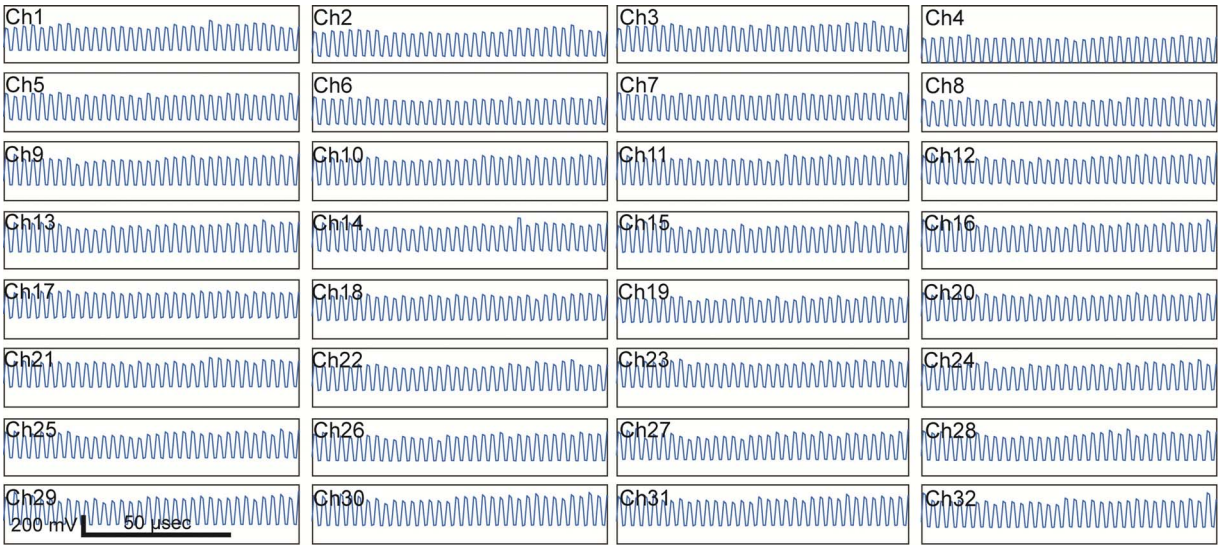

Fig. 5. The parallel recording of 32-ch ADCs at 1.3 MHz sampling rate per channel using the data acquisition system. Each measurement shows individual column outputs from the CMOS device. All 32 outputs contain time-division multiplexed signals from 1024 electrodes. Each square-wave period corresponds to the output of an individual electrode.

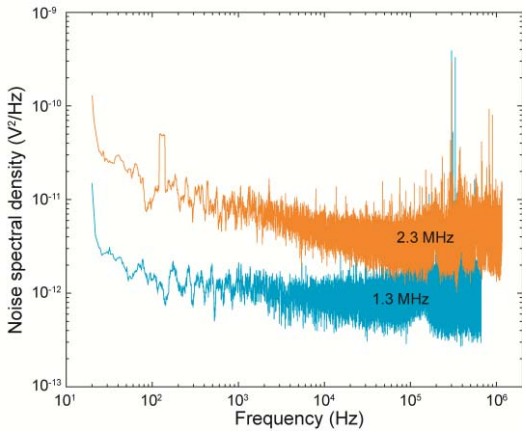

Fig. 6. The NSD of the multifunctional data acquisition system at two different sampling rate settings: 1.3 MHz and 2.3 MHz. The measured average noise levels are 1.01×10^{-12} V^2/Hz and 4.58×10^{-12} V^2/Hz for each sampling rate.

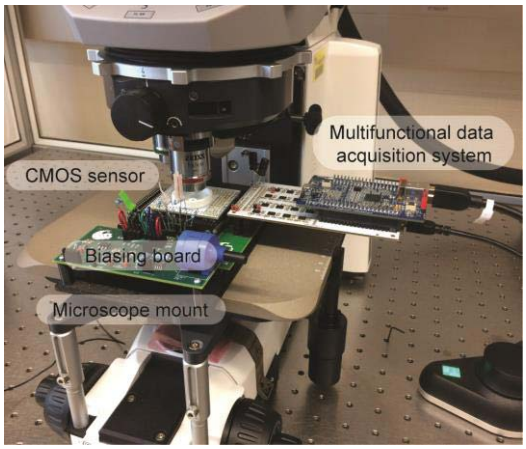

Fig. 7. Electrochemical imaging setup consisting of multifunctional data acquisition system, monolithic CMOS sensor, biasing board for the CMOS device, and a 3D-printed microscope mount for the system.

sampling rate of the multifunctional data acquisition system is 42.52 MHz. The electrochemical imaging is performed by measuring the oxidation of dopamine molecules at each electrode. For this experiment, the 3D-printed well is initially filled with 2 mL of phosphate buffered saline (PBS) and an Ag|AgCl reference electrode is inserted into the PBS solution. After the recording is started, 20 μL of 10-mM dopamine solution is injected into the well. This is expected to result in a 100-μM dopamine solution in the well by diffusion.

Electrodes located in the outer perimeter of the electrode array are covered by PDMS to deactivate their sensitivity to dopamine molecules (Fig. 8a). These electrodes are used as a control in this experiment to monitor the stable operation of overall circuits and electronics. Although these PDMS-covered electrodes are insensitive to the dopamine injection, they are functional in terms of recording capability and data processing. Any activity recorded in these electrodes may indicate the electrostatic injection of electrons or malfunction of the underlying circuits. Thus, the control can be used to isolate dopamine responses from any artifacts exhibited in recordings from uncovered electrodes. Dopamine oxidation is successfully measured from the electrodes which are not covered by PDMS (Fig. 8b). As configured by the multifunctional data acquisition system, a 2D electrochemical imaging of dopamine oxidation with over 10,000 frames per second is achieved (Fig. 8b and 8c). As a large concentration of dopamine reaches the electrodes, a significant increase in oxidation current is observed. A set of 32 electrochemical measurements from 7th row from the bottom of the array is shown in Fig. 8b. The visual inspection of the microphotograph in Fig. 8a indicates that 16 electrodes (columns 1 – 8 and 25 – 32) are covered by PDMS and the remaining 16 electrodes (columns 9 – 24)

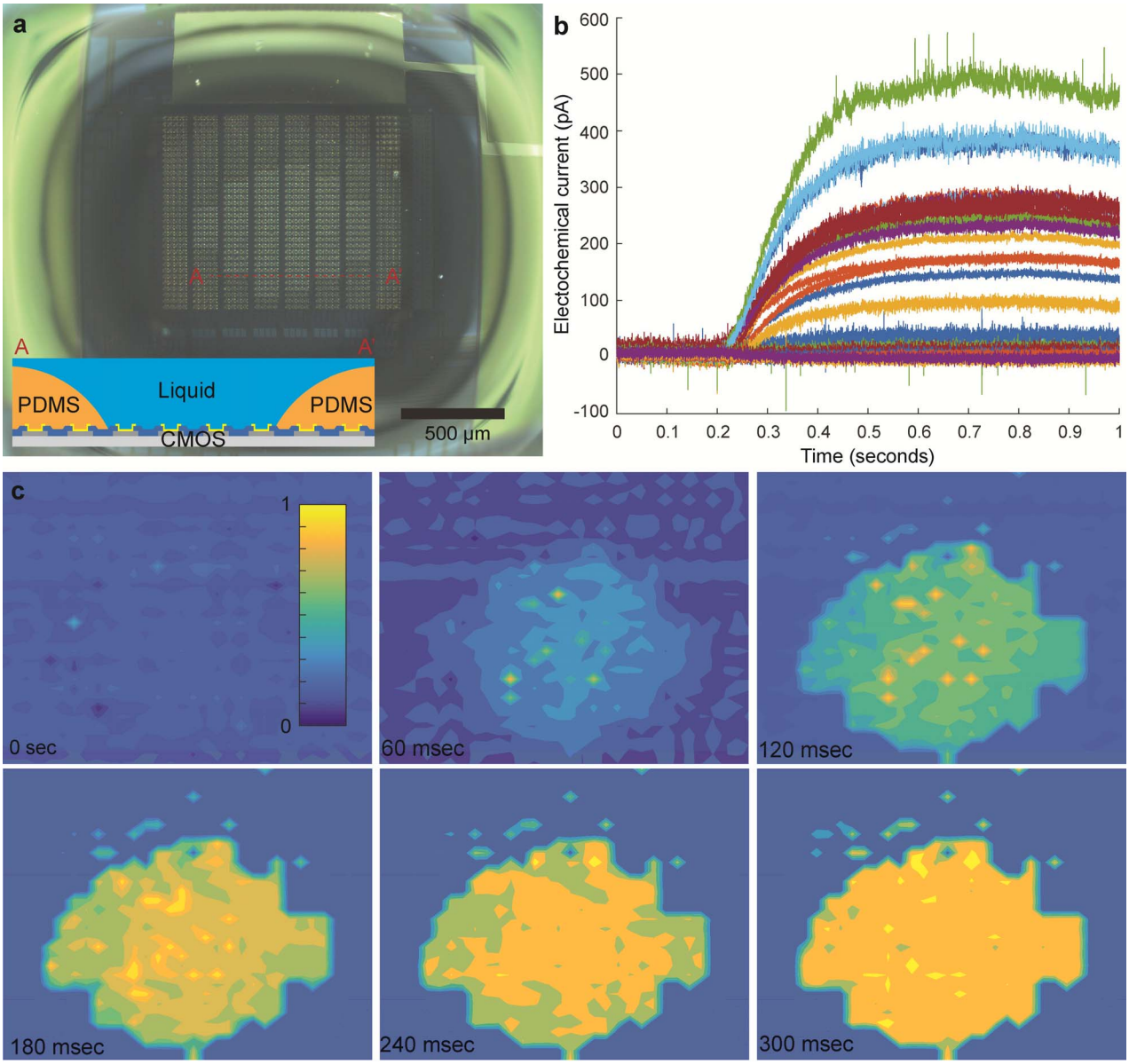

Fig. 8. The electrochemical imaging using the monolithic CMOS imaging sensor and multifunctional data acquisition system. (a) The microphotograph of the monolithic sensor with PDMS. Electrodes on the perimeter of the 1024 array are covered with PDMS to impede the dopamine measurement on those electrodes so that they can used as a control. The electrodes toward the middle, which are brighter in color, are open for dopamine measurements. (b) Electrochemical recordings from the 7th row from the bottom of the array. Each color corresponds to a different column of the measured row. (c) Diffusion of dopamine throughout the array in a 300ms time frame is shown at six selected frames, at 60 ms intervals, out of the 3000 recorded frames.

are not affected by PDMS in the 7th row from the bottom. As expected, the 16 uncovered electrodes (columns 9 – 24) exhibited dopamine responses over 50 pA, while the rest show little or no response (< 35 pA) to the dopamine injection.

The spatial diffusion of dopamine is visualized by 2D plotting the recordings of individual electrodes. Contour plots with filled color are generated for each frame, which includes all 1024 electrodes' current responses at each time point. Overall, 380 electrodes have detected the dopamine influx with responses over 50 pA. For the 2D plotting, a normalization is performed for the dopamine-sensitive electrodes. Six frames, out of 3000 frames recorded for a 300-ms measurement, with a 60-ms interval are presented in Fig. 8c. In the 0-ms frame, none of the electrodes in the array are sensing the oxidation of dopamine. At the 60-ms frame, electrodes in the center of the array are starting to detect the oxidation current, indicating the increase in the dopamine concentration near the array due to the dopamine injection in the 3D-printed well. In the following frames (120-ms, 180-ms, and 240-ms), the level of detection sharply increases, and most of the electrodes reach a steady-state at 300 ms. The steady-state is due to the slow diffusion of dopamine toward the electrode array compared to the quick oxidative consumption of dopamine by the electrodes [1]. Thus, the oxidation current reaches a diffusion-limited steady-state.

VI. Conclusion

In this paper, we present an electrochemical imaging platform that is comprised of a monolithic CMOS electrochemical sensor and a multifunctional data acquisition system that enables the system's high-throughput capability of over 10,000 frames per second. The multifunctional data acquisition system can potentially be used for other high-through applications with high versatility by reconfiguring the functions of most I/Os and the sampling rate of the ADCs.

Acknowledgment

The authors thank Edward Dein for his technical assistance in the clean room. Post-CMOS processing was carried out in Advanced Microfabrication Facility (AMPAC) at the University of Central Florida. Also, the authors thank the technical support team, Denise Tjon Ket Tjong, Steven Dick, and Derrick McQuern, in College of Engineering and Computer Science at University of Central Florida for their excellent support in maintaining the lab computers and file server used for this research project.

References

[1] B. N. Kim, A. D. Herbst, S. J. Kim, B. A. Minch, and M. Lindau, "Parallel recording of neurotransmitters release from chromaffin cells using a 10×10 CMOS IC potentiostat array with on-chip working electrodes," *Biosensors Bioelectron.*, vol. 41, pp. 736–744, Mar. 2013.

[2] N. Kasai, A. Shimada, T. Nyberg, and K. Torimitsu, "An electrochemical sensor array and its application to real-time brain slice imaging," *Electron. Commun. Jpn.*, vol. 92, no. 9, pp. 1–6, Sep. 2009.

[3] M. K. Zachek, P. Takmakov, J. Park, R. M. Wightman, and G. S. McCarty, "Simultaneous monitoring of dopamine concentration at spatially different brain locations *in vivo*," *Biosensors Bioelectron.*, vol. 25, no. 5, pp. 1179–1185, Jan. 2010.

[4] D. L. Bellin, H. Sakhtah, Y. Zhang, A. Price-Whelan, L. E. Dietrich, and K. L. Shepard, "Electrochemical camera chip for simultaneous imaging of multiple metabolites in biofilms," *Nature Commun.*, vol. 7, p. 10535, Jan. 2016.

[5] T. Tokuda, K. Tanaka, M. Matsuo, K. Kagawa, M. Nunoshita, and J. Ohta, "Optical and electrochemical dual-image CMOS sensor for on-chip biomolecular sensing applications," *Sens. Actuators A, Phys.*, vol. 135, no. 2, pp. 315–322, Apr. 2007.

[6] M. M. Rahman, A. Umar, and K. Sawada, "Development of amperometric glucose biosensor based on glucose oxidase co-immobilized with multi-walled carbon nanotubes at low potential," *Sens. Actuators B, Chem.*, vol. 137, no. 1, pp. 327–333, Mar. 2009.

[7] S. Takenaga, Y. Tamai, K. Okumura, M. Ishida, and K. Sawada, "Label-free acetylcholine image sensor based on charge transfer technology for biological phenomenon tracking," *Jpn. J. Appl. Phys.*, vol. 51, no. 2R, p. 27001, Jan. 2012.

[8] A. Hassibi and T. H. Lee, "A programmable 0.18-μm CMOS electrochemical sensor microarray for biomolecular detection," *IEEE Sensors J.*, vol. 6, no. 6, pp. 1380–1388, Dec. 2006.

[9] V. Viswam *et al.*, "Multi-functional microelectrode array system featuring 59,760 electrodes, 2048 electrophysiology channels, impedance and neurotransmitter measurement units," in *IEEE Int. Solid-State Circuits Conf. (ISSCC) Dig. Tech. Papers*, vol. 59, Jan./Feb. 2016, pp. 394–396.

[10] J. Dragas *et al.*, "*In vitro* multi-functional microelectrode array featuring 59 760 electrodes, 2048 electrophysiology channels, stimulation, impedance measurement, and neurotransmitter detection channels," *IEEE J. Solid-State Circuits*, vol. 52, no. 6, pp. 1576–1590, Jun. 2017.

[11] P. Shields, B. Nemeth, R. B. Green, M. O. Riehle, and D. R. S. Cumming, "High-speed imaging of 2-D ionic diffusion using a 16×16 pixel CMOS ISFET array on the microfluidic scale," *IEEE Sensors J.*, vol. 12, no. 9, pp. 2744–2749, Sep. 2012.

[12] J. Rothe, O. Frey, A. Stettler, Y. Chen, and A. Hierlemann, "Fully integrated CMOS microsystem for electrochemical measurements on 32 × 32 working electrodes at 90 frames per second," *Anal. Chem.*, vol. 86, no. 13, pp. 6425–6432, Jul. 2014.

[13] J. P. Grinias, J. T. Whitfield, E. D. Guetschow, and R. T. Kennedy, "An inexpensive, open-source USB Arduino data acquisition device for chemical instrumentation," *J. Chem. Educ.*, vol. 93, no. 7, pp. 1316–1319, Jul. 2016.

[14] D. Hercog and B. Gergič, "A flexible microcontroller-based data acquisition device," *Sensors*, vol. 14, no. 6, pp. 9755–9775, Jun. 2014.

[15] F. J. Ferrero Martín, M. V. Llopis, J. C. C. Rodríguez, J. R. B. González, and J. M. Blanco, "Low-cost open-source multifunction data acquisition system for accurate measurements," *Measurement*, vol. 55, pp. 265–271, Sep. 2014.

[16] J. P. Kinney *et al.*, "A direct-to-drive neural data acquisition system," *Front. Neural Circuits*, vol. 9, p. 46, Sep. 2015.

[17] R. Rajpal *et al.*, "Embedded multi-channel data acquisition system on FPGA for Aditya Tokamak," *Fusion Eng. Des.*, vol. 112, pp. 964–968, Nov. 2016.

[18] D. A. Borton, M. Yin, J. Aceros, and A. Nurmikko, "An implantable wireless neural interface for recording cortical circuit dynamics in moving primates," *J. Neural Eng.*, vol. 10, no. 2, p. 26010, Apr. 2013.

[19] J. Dunlop, M. Bowlby, R. Peri, D. Vasilyev, and R. Arias, "High-throughput electrophysiology: An emerging paradigm for ion-channel screening and physiology," *Nature Rev. Drug Discovery*, vol. 7, no. 4, pp. 358–368, Apr. 2008.

[20] J. S. Park *et al.*, "1024-pixel CMOS multimodality joint cellular sensor/stimulator array for real-time holistic cellular characterization and cell-based drug screening," *IEEE Trans. Biomed. Circuits Syst.*, vol. 12, no. 1, pp. 80–94, Feb. 2018.

[21] J. Rosenstein, M. Wanunu, C. A. Merchant, M. Drndic, and K. L. Shepard, "Integrated nanopore sensing platform with sub-microsecond temporal resolution," *Nature Methods*, vol. 9, no. 5, pp. 487–492, May 2012.

[22] K. Kisler *et al.*, "Transparent electrode materials for simultaneous amperometric detection of exocytosis and fluorescence microscopy," *J. Biomater. Nanobiotechnol.*, vol. 3, no. 2, pp. 243–253, May 2012.

Kevin A. White, photograph and biography not available at the time of publication.

Geoffrey Mulberry, photograph and biography not available at the time of publication.

Brian N. Kim, photograph and biography not available at the time of publication.